Molecular Physics
Vol. 110, No. 18, September 2012, 2295–2300

Taylor & Francis
Taylor & Francis Group

RESEARCH ARTICLE

Ab initio study of Ru-terminated and Ru-doped armchair graphene nanoribbons

B. Sarikavak-Lisesivdin[a]*, S.B. Lisesivdin[a] and E. Ozbay[bc]

[a]*Department of Physics, Faculty of Science, Gazi University, 06500 TeknikokullarAnkara, Turkey;* [b]*Bilkent University, Nanotechnology Research Center, 06800 Bilkent, Turkey;* [c]*Department of Physics, Department of Electrical and Electronics Engineering, Bilkent University, 06800 Bilkent, Turkey*

(*Received 20 January 2012; final version received 15 March 2012*)

We investigate the effects of ruthenium (Ru) termination and Ru doping on the electronic properties of armchair graphene nanoribbons (AGNRs) using first-principles methods. The electronic band structures, geometries, density of states, binding energies, band gap information, and formation energies of related structures are calculated. It is well founded that the electronic properties of the investigated AGNRs are highly influenced by Ru termination and Ru doping. With Ru termination, metallic band structures with quasi-zero-dimensional, one-dimensional and quasi-one-dimensional density of states (DOS) behavior are obtained in addition to dominant one-dimensional behavior. In contrast to Ru termination, Ru doping introduces small but measurable (12.4 to 89.6 meV) direct or indirect band gaps. These results may present an additional way to produce tunable band gaps in AGNRs.

Keywords: ruthenium; doping; termination; passivation

1. Introduction

The band structure of graphene, consisting of a few layers of graphite, was one of the first structures investigated theoretically [1]. With its free-standing two-dimensional structure, graphene is believed to be thermodynamically unstable under ambient conditions [2]. Interest in this material increased after the experimental study presented by Novoselov *et al*. [3]. Several fabrication methods have been reported [4–6] since the publication of the exfoliation method of Novoselov *et al*. These new fabrication methods have resulted in the production of the more successfully controlled quasi-one-dimensional form, the graphene nanoribbon (GNR) [7].

The electronic properties of GNRs are ruled by the size of the ribbon and the geometry along the edges [8]. Similar to zig-zag carbon nanotubes (CNTs), armchair-edged GNRs show semiconductor behavior and, like armchair CNTs, most of the zig-zag-edged graphene nanoribbons (ZGNRs) are metallic [9]. With a doping defect or edge defects, one can break the degeneracy of the spin polarization and make ZGNRs into half-metals or spin gapless semiconductors [10–12]. Kobayashi *et al*. observed a high density of edge states near the Fermi level for hydrogen-terminated graphite edges using scanning tunneling microscopy, which also verified experimentally the importance of edge states for GNRs [13]. Theoretical studies are mostly directed towards hydrogen-terminated GNRs, and there are a few examples of the different termination possibilities [14].

Graphene synthesis on non-carbide substrates using epitaxial methods has been studied to synthesize better graphene layers than when using the carbide sublimation method [15]. Very recent results have been reported with transition metal (TM) substrates such as Ni [6], Cu [16], and Ru [15]. Ru thin films have some advantages over Ni and Cu with their low-defect macroscopic crystalline domains, which result in successful thickness control on Ru (0001) substrates [15,17]. Because of these advantages, understanding the interaction of graphene and the transition metals Ni [18], Cu and Ru is of great importance. Several theoretical studies on graphene-on-Ru substrates [19–23] have been reported in order to understand this interaction. These studies all concern graphene-on-Ru substrates and provide very little, or no, information on Ru-terminated or Ru-doped graphene structures.

In the present study, we investigated the electronic properties of Ru-terminated and highly Ru-doped AGNRs using density-functional-theory (DFT) calculations.

*Corresponding author. Email: beyzas@gazi.edu.tr

ISSN 0026–8976 print/ISSN 1362–3028 online

http://dx.doi.org/10.1080/00268976.2012.678905
http://www.tandfonline.com

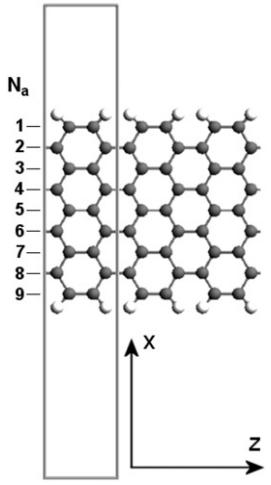

Figure 1. Supercell of the 9-AGNR structure. This structure is hydrogenated. Gray and white atoms represent carbon and hydrogen, respectively. Ribbons are allowed to grow only in the z-direction. The other two axes are confined.

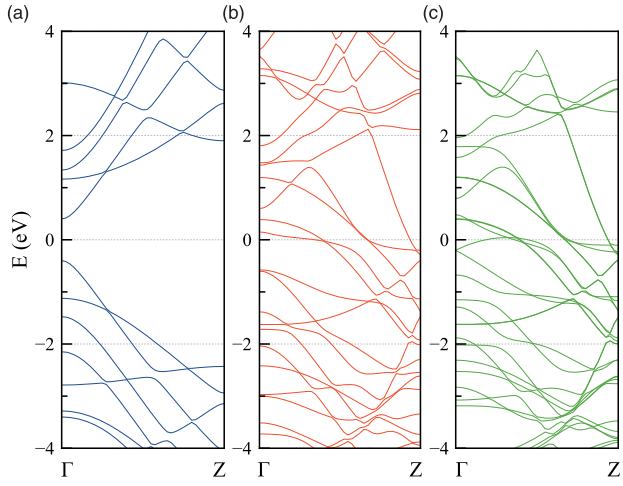

Figure 2. Band structures of (a) H-terminated, (b) single-side Ru-terminated and (c) both side Ru-terminated structures.

2. Computational method

The calculations were performed using the Atomistix Toolkit – Visual NanoLab (ATK-VNL) [24–26]. As an exchange correlation function, the local density approximation (LDA) was used in the form of Perdew and Zunger [27]. Periodic boundary conditions for the z-axis and vacuum confinement for the x- and y-axes are utilized. For the vacuum confinement region, the intervals among the ribbons were kept sufficiently spaced to ensure minimization of the interaction between two periodic slabs. An energy cut-off value of 100 Ry was selected to ensure accurate results. Brilliouin zone integration was performed with a regular Monkhorst–Pack $1 \times 1 \times 100$ k-point grid [28]. All atoms were fully relaxed and maximum force components on all atoms were accepted to be less than 0.005 eVÅ^{-1}. We refer to armchair GNR with N_a dimer lines as N_a-AGNR. We examined symmetrical AGNRs with widths of $N_a = 7$–11, but since the results are similar, we only present the results for 9-AGNRs. In our calculations, we modeled AGNRs with one side Ru-terminated and one side H-terminated, both sides Ru-terminated, and Ru-doped as a dimer line, which is again referred to as N_a. It may be more convenient to explain doping as alloying due to the number of atoms. Figure 1 shows the modeled structure and the supercell used for the simulation.

3. Results and discussion

Calculations were performed for bare, H-terminated, single-side Ru-terminated, both sides Ru-terminated and Ru-doped with various configurations for different ribbon widths ($N_a = 7$–11) and the effects of spin. In our calculations, we obtain the same degenerate results for spin-included cases, which is related to the investigated AGNRs with or without Ru atoms being non-magnetic. We present the results for $N_a = 9$ below for simplicity.

3.1. *Effects of Ru termination*

The band structures of bare, H-terminated, single-side Ru-terminated, both sides Ru-terminated and Ru-doped cases were obtained in order to understand the nature of the interaction of Ru with the AGNRs. In our bare ribbons, there are four edge carbons with one dangling bond per edge carbon atom. We observed that these dangling bonds result in a decrease in the lattice parameters as well as indirect semiconductor behavior, which is compatible with the literature [29]. The H-terminated structure shown in Figure 2(a) gives a direct band gap that demonstrates the expected semiconductor behavior. The structure with single-side Ru-termination, shown in Figure 2(b), has additional delocalized 4d states from Ru atoms that impart metallic nature to the structure. It should be pointed out that spin-up and spin-down states are degenerate. Figure 2(c) shows the band structure of the both-sides Ru-terminated structure. The band structure is similar to the single-side Ru-terminated case, but with a difference in the nature of the folding. This behavior is expected due to the symmetrical nature of the terminations. Therefore, the number of conducting states crossing the Fermi level is doubled with the additional Ru termination of a single side.

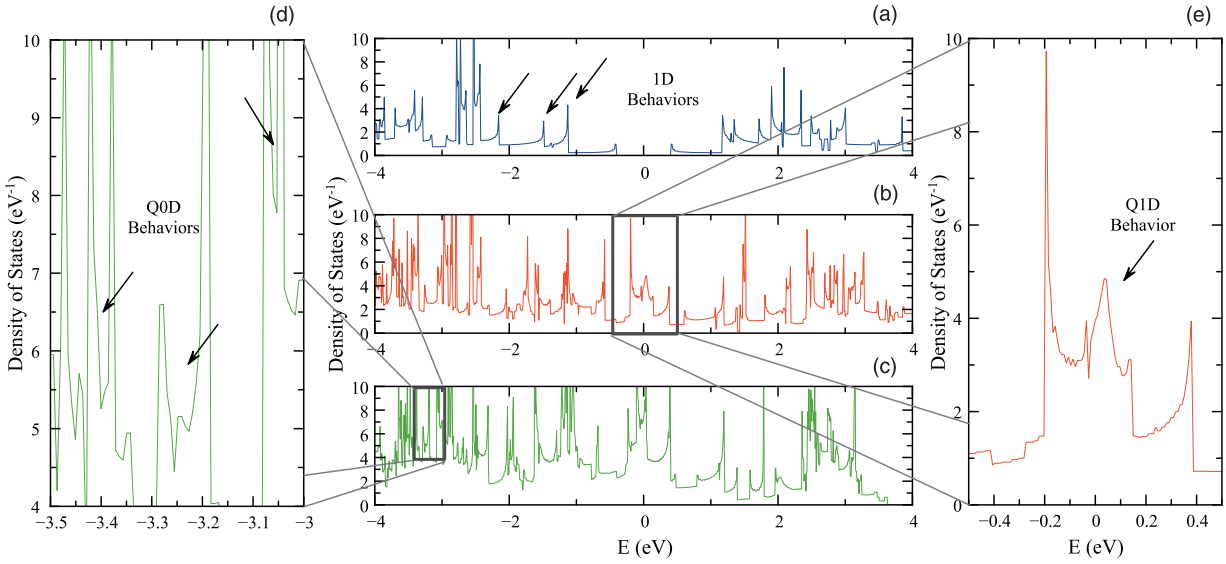

Figure 3. The DOS data of (a) H-terminated, (b) single-side Ru-terminated and (c) both side Ru-terminated structures. Detailed views of Q0D and Q1D DOS peaks for (d) both-side Ru-terminated and (e) single-side Ru-terminated structures.

The density of states (DOS) of these structures is shown in Figure 3(a)–(c). The DOS of the H-terminated structure, shown in Figure 3(a), presents the well-known symmetric one-dimensional (1D) DOS behavior with a band gap of 0.80 eV. The structures with single-side Ru-termination and both side Ru-termination do not present a band gap due to the hybridization between C-p and Ru-4d orbitals. The DOS of the structure with single-side Ru-termination (Figure 3(b)) near the Fermi level shows local quasi-one-dimensional (Q1D) behavior [30]. In addition to this local behavior, many types of expected 1D DOS behavior were observed. In addition, the DOS spectrum of the both side Ru-terminated structure exhibits many types of quasi-zero-dimensional (Q0D) behavior, as shown in Figure 3(c) [30]. The origin of this behavior is unknown. Figure 3(d) and (e), which show parts of Figures 3(c) and (b) in more detail, clearly show the Q0D and Q1D DOS peaks.

In addition to the band structures and DOS, we calculated the related binding energies (BE) of the investigated structures. For the bare ribbon and other terminated configurations, the BE is calculated as

$$E_B = \frac{E_{T,\,Bare}}{n} - E_C \quad \text{(for bare)} \tag{1}$$

and

$$E_B = E_T - E_{T,\,Bare} - nE_H - mE_{Ru} \quad \text{(for other configurations)}, \tag{2}$$

respectively. Here, E_B, E_T, $E_{T,Bare}$, E_C, E_H, E_{Ru}, n and m are the BE, the total energy of the investigated configuration, the total energy of bare AGNR, the total energy of isolated carbon, hydrogen and ruthenium atoms, the number of hydrogen atoms and the number of ruthenium atoms, respectively. A lower energy corresponds to stronger binding of the atoms. The calculated BEs for the investigated configurations are listed in Table 1. In contrast to Cu-terminated and Ni-terminated AGNRs [14,29], both-side Ru-terminated structures are the most stable followed by single-side Ru-terminated and H-terminated structures, which shows a notable interaction between Ru and C atoms at the edges.

Table 1. Binding energy per carbon atom of related configurations.

	Binding energy per C atom (eV)
Bare ribbon	−0.556
H-terminated	−1.307
Single-side Ru-terminated	−1.629
Both side Ru-terminated	−1.953

3.2. *Effects of Ru doping*

The interaction between Ru and C atoms at the edges raises the question of the effects of Ru doping in these structures. In order to investigate these effects, we doped the H-terminated structure with Ru at the dimer lines shown as N_a in Figure 1. Figure 4(a)–(f) show the band structures of the H-terminated structure and

doped structures with $N_a = 1$–5. Structures with $N_a = 6$–9 are not included due to the symmetry of the structure. As can be seen from Figure 4, new states arise at both the conduction and valance bands due to the strong interaction of Ru with C, but we do not observe any Fermi level crossing due to the doping line. Changes in band structures increasingly decrease with doping towards the center of the ribbon. All the investigated doping lines ($N_a = 1$–5) show direct or indirect band gaps. Table 2 reports the properties of these band gaps. According to these values, the H-terminated structure and structures with $N_a = 2$ and 5 show direct semiconductor behavior, and the other structures show somewhat indirect behavior. The H-terminated structure has a known direct band gap value of 0.80 eV, which is compatible with the literature value of 0.75 eV [12]. With Ru doping at dimer lines $N_a = 1$–5, various band gaps of 12.4 to 89.6 meV are obtained. These values are open to discussion and a further detailed investigation with different exchange potentials and geometries is recommended. Because these band gaps are on the meV scale, Figures 4(a)–(f) show the details near the Fermi level and these band gaps can clearly be observed in Figure 5(a)–(f).

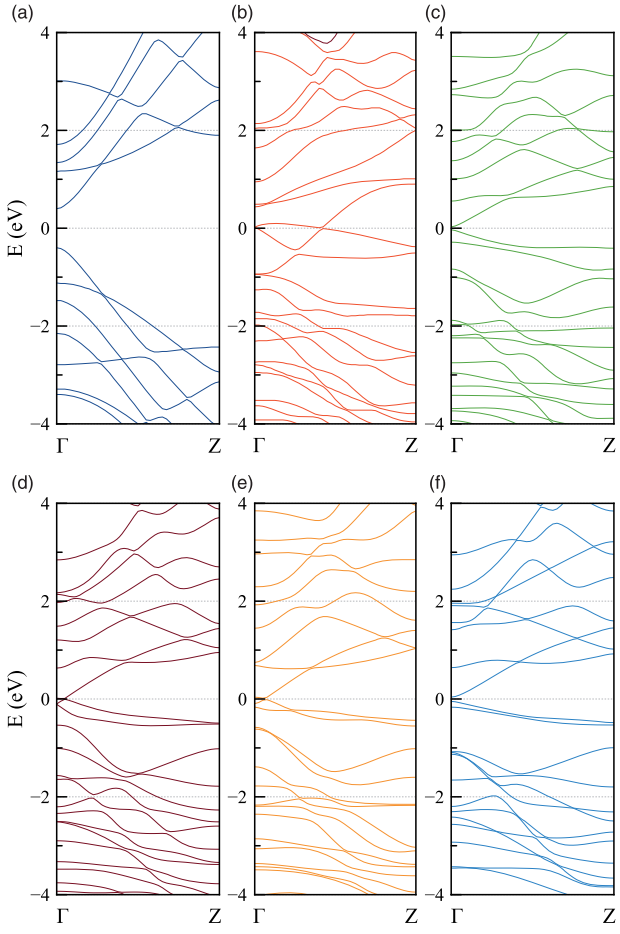

Figure 4. Band structures of the H-terminated structure (a) and doped structures with $N_a = 1$–5 ((b)–(f)).

In order to determine which of these configurations is energetically favorable, we calculated the formation energy [31]:

$$E_{\text{Form}} = (E_T + nE_C) - (E_{T,H} + nE_{Ru}), \qquad (3)$$

where $E_{T,H}$ is the energy of the H-terminated configuration and n is the number of Ru atoms, which is two in the investigated structures. Calculated formation energies are shown in Figure 6. Structures with doping lines $N_a = 1$ and 9 are energetically the most favorable. In addition, the structure with doping line $N_a = 5$ is energetically favorable with respect to lines $N_a = 3$, 4, 6, and 7. The behavior of line $N_a = 5$ can mostly be attributed to the symmetry of the structure, and the contributions of both symmetric parts are favored at the center. Generally, it can be stated that Ru doping near the edges is energetically favorable with respect to the other doping lines.

4. Conclusion

In summary, we have performed first-principles calculations to study the geometries and electronic

Table 2. Valance band maximum, conduction band minimum, band gap, and type of band gap of H-terminated and doped structures.

Structure	Valence band maximum (eV)	Conduction band minimum (eV)	Band gap (eV)	Direct gap
H-terminated	−0.4006	0.4006	0.8013	Yes
Dope at dimer line $N_a = 1$	−0.0067	0.0057	0.0124	No
Dope at dimer line $N_a = 2$	−0.0356	0.0303	0.0658	Yes
Dope at dimer line $N_a = 3$	−0.0049	0.0103	0.0152	No
Dope at dimer line $N_a = 4$	−0.0175	0.0167	0.0342	No
Dope at dimer line $N_a = 5$	−0.0496	0.0400	0.0896	Yes

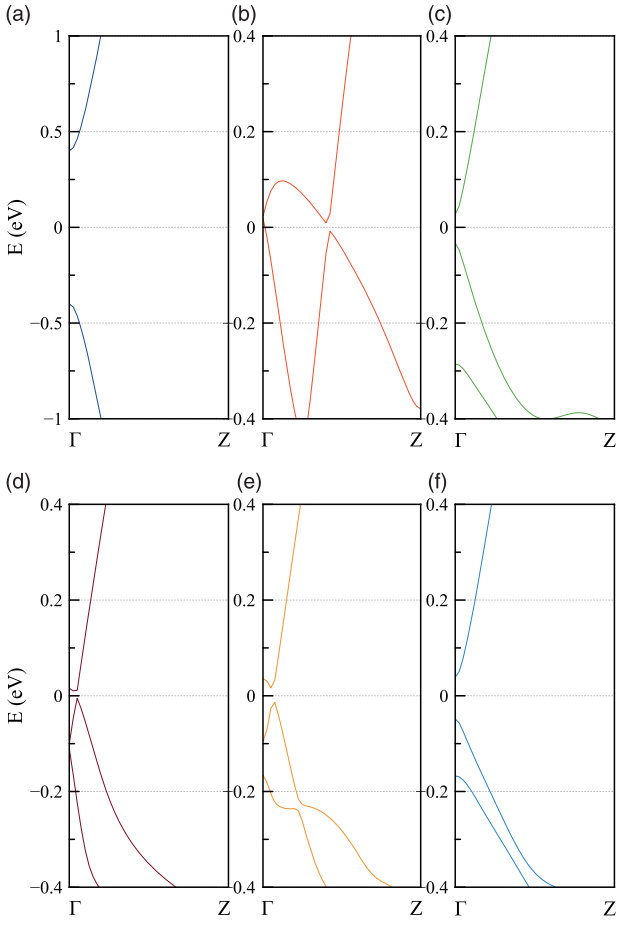

Figure 5. Band gap formation in the H-terminated structure (a) and doped structures with $N_a = 1$–5 ((b)–(f)).

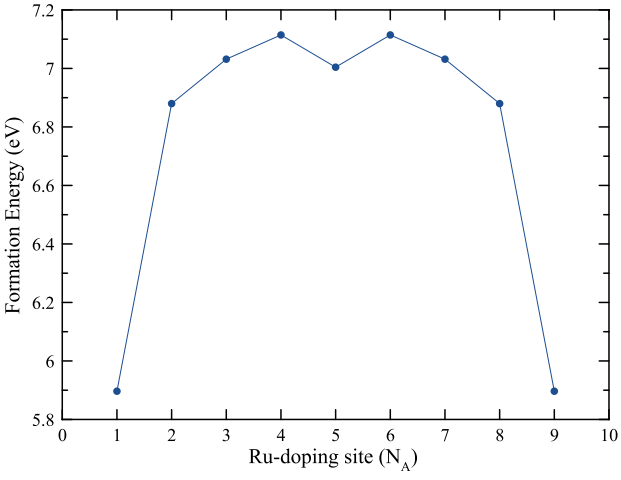

Figure 6. Formation energies for Ru-doped 9-AGNR structures for different sites.

structures of armchair graphene nanoribbons with Ru atom termination and Ru doping. We found that Ru termination can significantly influence the electronic properties of AGNRs, induce metallicity and introduce Q0D- and Q1D-type states in addition to 1D states. In contrast to Ru termination, small direct or indirect band gaps with values of 12.4 to 89.6 meV are maintained with Ru doping. These results are important figures of merit in order to obtain tunable band gaps experimentally with graphene. Future first-principles and experimental studies could find a definite answer to the band gap modifying effect of Ru atoms in the graphene lattice, which is, however, beyond the scope of the present paper.

Acknowledgements

This work is supported by the State Planning Organization of Turkey under grant No. 2011K120290, by the projects DPT-HAMIT, ESF-EPIGRAT, EU-N4E, and NATO-SET-181, and TUBITAK under project Nos. 107A004, 107A012, and 109E301. One of the authors (E.O.) also acknowledges partial support from the Turkish Academy of Sciences. We kindly thank Dr. Pankaj Srivastava from the Indian Institute of Information Technology and Management for the fruitful discussion.

References

[1] P.R. Wallace, Phys. Rev. **71**, 622 (1947).
[2] N.D. Mermin and H. Wagner, Phys. Rev. Lett. **17**, 1133 (1966).
[3] K.S. Novoselov, A.K. Geim, S.V. Morozov, D. Jiang, Y. Zhang, S.V. Dubonos, I.V. Grigorieva and A.A. Firsov, Science **306**, 666 (2004).
[4] C. Berger, Z. Song, T. Li, X. Li, A.Y. Ogbazghi, R. Feng, Z. Dai, A.N. Marchenkov, E.H. Conrad, P.N. First and W.A. de Heer, J. Phys. Chem. B **108**, 19912 (2004).
[5] S. Stankovich, D.A. Dikin, G.H.B. Dommett, K.M. Kohlhaas, E.J. Zimney, E.A. Stach, R.D. Piner, S.T. Nguyen and R.S. Ruoff, Nature **442**, 282 (2006).
[6] L.G. De Arco, Y. Zhang, A. Kumar and C. Zhou, IEEE Trans. Nanotechnol. **8**, 135 (2009).
[7] X. Li, X. Wang, L. Zhang, S. Lee and H. Dai, Science **319**, 1229 (2008).
[8] S.S. Yu, Q.B. Wen, W.T. Zheng and Q. Jiang, Molec. Simul. **34**, 1085 (2008).
[9] Y.W. Son, M.L. Cohen and S.G. Louie, Phys. Rev. Lett. **97**, 216803-1 (2006).
[10] Y. Li, Z. Zhou, P. Shen and Z. Chen, ACS Nano **3**, 1952 (2009).
[11] S. Lakshmi, S. Roche and G. Cuniberti, Phys. Rev. B **80**, 193404 (2009).
[12] U. Treske, F. Ortmann, B. Oetzel, K. Hannewald and F. Bechstedt, Phys. Stat. Sol. A **207**, 304 (2010).

[13] Y. Kobayashi, K.I. Fukui, T. Enoki and K. Kusakabe, Phys. Rev. B **73**, 125415-1 (2006).
[14] N.K. Jaiswal and P. Srivastava, Solid State Commun. **151**, 1490 (2011).
[15] P.W. Sutter, J.-I. Flege and E.A. Sutter, Nature Mater. **7**, 406 (2008).
[16] X. Li, W. Cai, J. An, S. Kim, J. Nah, D. Yang, R. Piner, A. Velamakanni, I. Jung, E. Tutuc, S.K. Banarjee, L. Colombo and R.S. Ruoff, Science **324**, 1312 (2009).
[17] K.L. Man and M.S. Altman, Phys. Rev. B **83**, 235415 (2011).
[18] M. Nahali and F. Gobal, Mol. Phys. DOI: 10.1080/00268976.2012.656719.
[19] D. Stradi, S. Barja, C. Diaz, M. Garnica, B. Borca, J.J. Hinarejos, D. Sanchez-Portal, M. Alcami, A. Arnau, A.L. Vazquez de Parga, R. Miranda and F. Martin, Phys. Rev. Lett. **106**, 186102 (2011).
[20] S. Saadi, F. Abild-Pedersen, S. Helveg, J. Sehested, B. Hinnemann, C.C. Appel and J.K. Nørskov, J. Phys. Chem. C **114**, 11221 (2010).
[21] B. Wang, S. Günther, J. Wintterlin and M.-L. Bocquet, New J. Phys. **12**, 043041 (2010).
[22] X. Peng and R. Ahuja, Phys. Rev. B **82**, 045425 (2010).
[23] D. Jiang, M.-H. Du and S. Dai, J. Chem. Phys. **130**, 074705 (2009).
[24] Version 11.8.2 QuantumWise A/S. <http://www.quantumwise.com>
[25] M. Brandbyge, J.-L. Mozos, P. Ordejón, J. Taylor and K. Stokbro, Phys. Rev. B **65**, 165401 (2002).
[26] J.M. Soler, E. Artacho, J.D. Gale, A. García, J. Junquera, P. Ordejón and D. Sánchez-Portal, J. Phys. Condens. Matter **14**, 2745 (2002).
[27] J.P. Perdew and A. Zunger, Phys. Rev. B **23**, 5048 (1981).
[28] H.J. Monkhorst and J.D. Pack, Phys. Rev. B **13**, 5188 (1976).
[29] N.K. Jaiswal and P. Srivastava, Physica E **44**, 75 (2011).
[30] H. Cho and P.R. Prucnal, J. Vac. Sci. Technol. B **7**, 1363 (1989).
[31] S.S. Yu, W.T. Zheng, Q.B. Wen and Q. Jiang, Carbon **46**, 537 (2008).